CrossMark

ORIGINAL ARTICLE

Investigation of groundwater chemistry at a dam site during its construction: a case study of Xiangjiaba Dam, China

Ji-Xiang Huo · Han-Zhou Song · Li Luo

Abstract Water quality can be used to reflect the hydro-geological features and seepage restrictions around grout curtains. Xiangjiaba Dam, a large hydropower station constructed in southwest of China, was investigated as a case study. Groundwater samples were collected and analysed qualitatively using hydrochemistry diagrams, after which the presence of four major water groups was determined by hierarchical cluster analysis and saturation indices of each group were calculated. Finally, inverse geochemical models of the groups were developed using PHREEQC to elucidate the dissolution/precipitation quality of different minerals and the relative contributions of different seepage sources. The hydro-geochemical methods used were found to be useful for revealing seepage behaviour within the domain during construction of a hydropower station.

Keywords Groundwater · Dam · Hydrochemistry · Cluster analysis · Inverse modelling

Introduction

Groundwater quality provides a wealth of information. The formation and evolution of groundwater reflect the geological and hydro-geological conditions of where it is located, as well as anthropogenic influences. Accordingly, groundwater investigations are used in many fields to identify hydro-geochemical processes and their relationship with groundwater quality (Hussein 2004; Kumar et al.

2006, 2009), develop models of groundwater flow paths for determination of recharge sources of recharge, the origin of solutes and the hydro-chemical evolution (Carucci et al. 2012; Sung et al. 2012), understand the impact of landfill leachate on groundwater quality (Srivastava and Ramanathan 2008) and investigate the release mechanism and sources of pollutants such as As (Sharif et al. 2008; Stüben et al. 2003) and fluoride (Chae et al. 2007; Salifu et al. 2012). Groundwater quality is also used to identify geochemical processes and the thermodynamic behaviour of dissolved and precipitated carbonate minerals in the seawater/freshwater mixing zone (Lin et al. 2013). Various methods have been applied to investigate geochemistry in the context of a site's groundwater hydrology. The use of various types of hydrochemistry diagrams can directly reflect water quality characteristics; however, this method has serious limitations when used alone (Güler et al. 2002). Multivariate statistical techniques such as descriptive statistical analysis, correlation analysis, cluster analysis and factor analysis can use any combination of chemical parameters to classify water samples (Cloutier et al. 2008; Dassi 2011; Gambillara et al. 2013; Kim et al. 2005; Mahlknecht et al. 2004; Monjerezi et al. 2011). Hydrogeochemical inverse modelling can be used to quantify the amounts of dissolution/precipitation that may interact with the groundwater (Belkhiri et al. 2010; Chae et al. 2006; Güler and Thyne 2004; Ma et al. 2011; Rosenthal et al. 2007). Such methods can directly reflect groundwater origins, supply sources and flow paths, as well as quantify the amount of mineral migration that occurs during concomitant water–rock interactions.

The construction of large hydropower projects leads to potentially irreversible changes in the region around the dam, such as those experienced by the flow field and chemical composition of groundwater. Over time, the

J.-X. Huo (✉) · H.-Z. Song · L. Luo
College of Earth Science and Engineering, Hohai University, Nanjing 210098, China
e-mail: jixianghuo@hotmail.com

curtain of the dam's foundation or abutments may weaken because of interactions between water and the local solid phases, leading to an increased risk of leakage. Various measures in addition to evaluation of the geological and hydro-geological conditions in the region are commonly used to investigate site conditions, including drilling, coloured tracer dyes, measurement of uplift pressure, seepage flow analysis and measurement of water chemistry composition (Ghobadi et al. 2005; Lee et al. 2005; Peng and Wang 2008; Unal et al. 2007; Uromeihy and Farrokhi 2012). Therefore, investigations of the basic dynamic characteristics of the groundwater regime around such dams are important to monitoring and understanding regional security risks and the development of appropriate remedial actions when necessary (Craig et al. 2007; Nusier et al. 2002). Some studies have analysed the in situ water chemistry of dams that have been in operation for various periods of time based on hydrochemistry diagrams and multivariate statistical methods (El Naqa and Al Kuisi 2004; Lee et al. 2009). Craft et al. (2007) concluded that the primary approach for interpreting seepage chemistry data during dam safety assessments should be as follows: (1) plotting available data on various types of hydrochemistry diagrams for visual comparison; (2) calculating mineral saturation indices for each sample; (3) calculating differences in data between seeps and reservoir concentrations; (4) determining the effects of mixing; (5) development of a geochemical mass balance model to help account for differences in data that are not attributable to mixing; (6) determining the amount of specific mineral dissolution reactions. However, the equipment for monitoring uplift pressure, seepage flow, etc. is not installed yet during the construction of hydropower stations. As a result, there are insufficient or no monitoring data available for formation of a time series to reflect the seepage conditions under the dam foundation. In such cases, water quality data and their analyses are particularly important.

In the present study, the Xiangjiaba Dam was used as a case study. During its construction, groundwater seepage was observed from the drill boreholes in the dam's foundation. To determine its source and potential impact, water samples were collected from upstream in the river, groundwater on both river banks and different parts of the dam foundation and subjected to chemical analysis, after which hydrochemistry diagrams representing the data were generated. Thereafter, a hierarchical clustering method was used to give a Q-cluster mode for all water samples so that water quality data could be sub-divided according to sample compositions. Finally, inverse modelling with PHREEQC was used to determine the proportion of seepage/leakage sources and the amount of each precipitation/dissolution mineral phase that may have arisen during the course of seepage. The significance of these measures was discussed and the induced changes in hydro-geological conditions during construction were assessed.

Project description

Xiangjiaba Dam, the third-largest hydropower station in China, is located on the Jinsha River, which is the upper stretch of the Yangtze River. The average discharge of the Jinsha River is about 4620 m^3/s. The dam is on the border between Yibin County, Sichuan Province and Shuifu County, Yunnan Province, southwest China (Fig. 1). Although the dam is mainly used to generate electricity, it is also designed to improve navigation conditions, control flooding, provide irrigation water and exert regulatory effects downstream. The dam primarily consists of water-retaining structures, flood discharge and energy dissipation structures, sediment washing buildings, a diversion and power system on its left bank, an underground diversion and power system on its right bank, navigation structures, irrigation water intakes and other components. The structure is a concrete gravity dam with a height to crest of 162 m and a length of 896.26 m. The water level upstream is assumed to be 380 m, and the total reservoir capacity is about 5.163 billion m^3. The facility has eight turbines, each with a capacity of 800 MW, giving a total generating capacity of 6400 MW.

Construction started in November 26, 2006, the first generator was commissioned in October 2012 and the project is scheduled to be completed in June 2015, taking a total of about 9 years and 6 months. The engineering construction used phased river diversion as follows: Phase I, circumvent the left bank, and build the non-overflow section of this side in the pit of this phase; Phase II, circumvent the right bank, and build the non-overflow section of this side, flood discharge section, stilling basin, plant on the left bank, ship lift, and ancillary buildings in the pit.

Geology and hydrology

The strata beneath the dam site mainly included the Triassic system upper series Xujiahe formation (T_{3xj}), the Triassic system middle series Leikoupo formation (T_2^1), the Jurassic system middle lower series Ziliujing formation (J_{1-2z}) and quaternary (Q) deposits. Among these, the outcropping bedrock of the dam site mainly included sandstone intercalated pelitic rocks of the Triassic system upper series Xujiahe formation (T_{3xj}), the red layer of the Jurassic system middle lower series Ziliujing formation (J_{1-2z}) on both sides and the slope of the leading channel

Fig. 1 *Map* showing the location of Xiangjiaba Dam

Fig. 2 General view of geological map of dam site and two cross sections
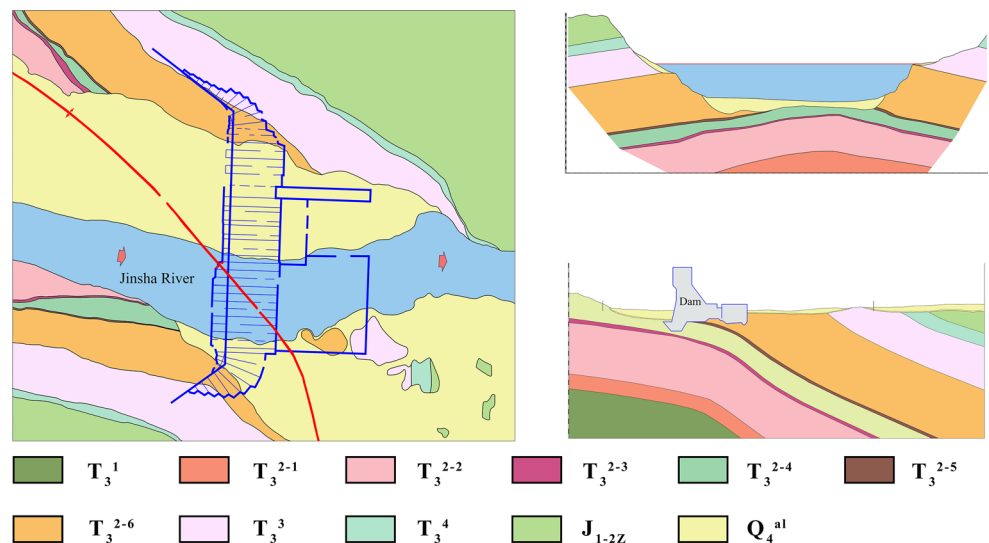
located on the downstream left bank and the Triassic system middle series Leikoupo formation (T_2^1) limestone buried below the dam (depth >260 m). The general geological setting of the site is shown in Fig. 2 and the description of the stratum is shown in Table 1.

The dam site is located in the eastern section of the Tangfangwan anticline. The anticline is the backbone structure of the dam area, which is dome shaped. Its core is located in the Jinsha River valley and its east and west ends plunge downward. The anticline extends through the entire dam length, which is about 6 km. Another geological structure is the Limeiwan deflection, which is a knee-shaped deflection that extends through the dam, with its occurrence of axis surface facing NW, trending toward SW and dipping 30°–40°. The fractured zone of deflection core is north–south trending, inclined downstream, with an inclination greater than 40°. Near the left bank are an extrusion fracture zone, some weak intercalations between layers, small faults and fissures.

According to the lithological characteristics and permeability differences between each rock group, the dam site area was divided into a relatively impermeable layer and an aquifer, with the former area mainly including the T_3^1, T_3^3 and J_{1-2Z} rock groups. Because of the presence of many more pelitic rocks, these groups have little water storage and poor permeability. The latter mainly included the T_3^2 and T_3^4 rock groups, which were primarily present in fine to coarse sandstones, with pore and fissure water flowing through cracks and fault fractures. Additionally, there was increased permeability in areas with more storage.

Table 1 Description of strata

Label	Strata	Characteristic	Thickness (m)
T_2^1	Triassic system middle series Leikoupo formation	Dolomitic mudstone and argillaceous dolomite at the bottom, limestone and dolomitic limestone at the top	180–234
T_3^1	Triassic system upper series Xujiahe formation	Grey and dark grey argillaceous siltstone, silty mudstone and mudstone with fine sandstone sandwich	≈ 105
T_3^{2-1}		Light grey thick sandstone, with argillaceous siltstone and siltstone on top, coal in some areas	25–30
T_3^{2-2}		Light grey thick sandstone, with thin fine sandstone sandwich and siltstone lens, coal in some areas	75–104
T_3^{2-3}		Grey and dark grey thin silty mudstone and argillaceous siltstone, with fine sandstone lens	2–1 3
T_3^{2-4}		Light grey thick sandstone, with thin fine sandstone and siltstone and silty mudstone lens	25–35
T_3^{2-5}		Dark grey thin silty mudstone and argillaceous siltstone and siltstone, with fine sandstone lens	0.5–8
T_3^{2-6}		Thick sandstone, with a few silty mudstone sandwiches and lenses	130–178
T_3^3		Sandstone, fine sandstone, siltstone, with a sandwich of seven thin coal layers	90–120
T_3^4		Light grey thin sandstone	15–35
J_{1-2z}	Jurassic system middle lower series Ziliujing formation	Thin argillaceous siltstone, silty mudstone and siltstone	251–254
Q_4	Quaternary	Gravel with sand sandwich	10–40

Based on the structural geology, lithological characteristics and hydro-geological information, the hydrogeology of this region could be sub-divided into an upper and lower aquifer. The upper aquifer mainly lies on both sides of the sandstone layer of the T_3^4 and T_3^3 and J_{1-2z}, presenting porosity with some small fractures. This aquifer is primarily recharged by atmospheric precipitation and shows obvious seasonal differences in level. This unconfined aquifer does not have a unified or stable groundwater level, and the amount of water in this aquifer is small. The bottom aquifer is primarily located on both sides of the lower part of the slope and the T_3^2 rock group of the river bed, the roof and floor of T_3^3 and the rock group of T_3^1, which may form the confined aquifer in some places. This aquifer is under the main part of the dam site and receives recharge from atmospheric precipitation and the upper aquifer. The groundwater level is located in the superficial part of the slope, where the river level was nearly horizontal and exhibits synchronous fluctuation. Observation during the period of geological survey revealed that the aquifer had close links to the river (Fig. 3).

Chemical analysis of the groundwater

During construction of the Xiangjiaba hydropower station, several different types of drilling were conducted at various locations in the dam foundation (e.g. curtain grouting
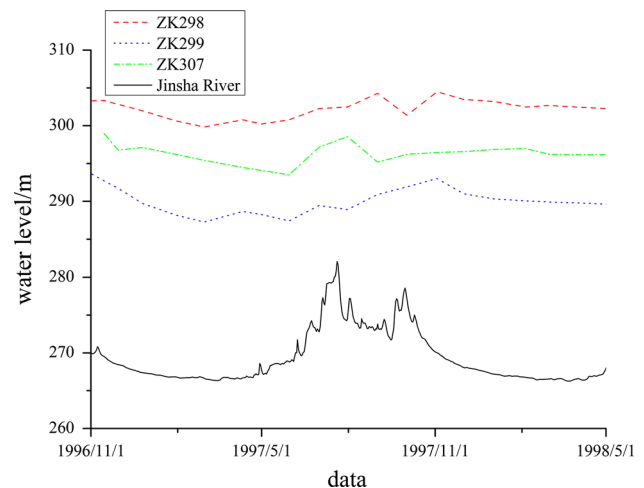
Fig. 3 Water level of Jinsha River and groundwater on both banks during the period of geological survey. ZK298 and ZK299 are observation boreholes on the *left* bank, while ZK307 is on the *right* bank

boreholes, curtain grouting inspection boreholes, drainage boreholes, reinforcing grout curtain boreholes, etc.) and seepage/leakage was observed in these boreholes during their formation. A cross section of the conceptual flow model during construction is shown in Fig. 4. It could be seen that the heads of upstream and downstream were 267.21 and 265.80 m, respectively. The water from the drainage boreholes flowed through the aquifer and the grout curtain. The seepage/leakage occurred mainly in the

Fig. 4 Sketch of the conceptual flow model during construction
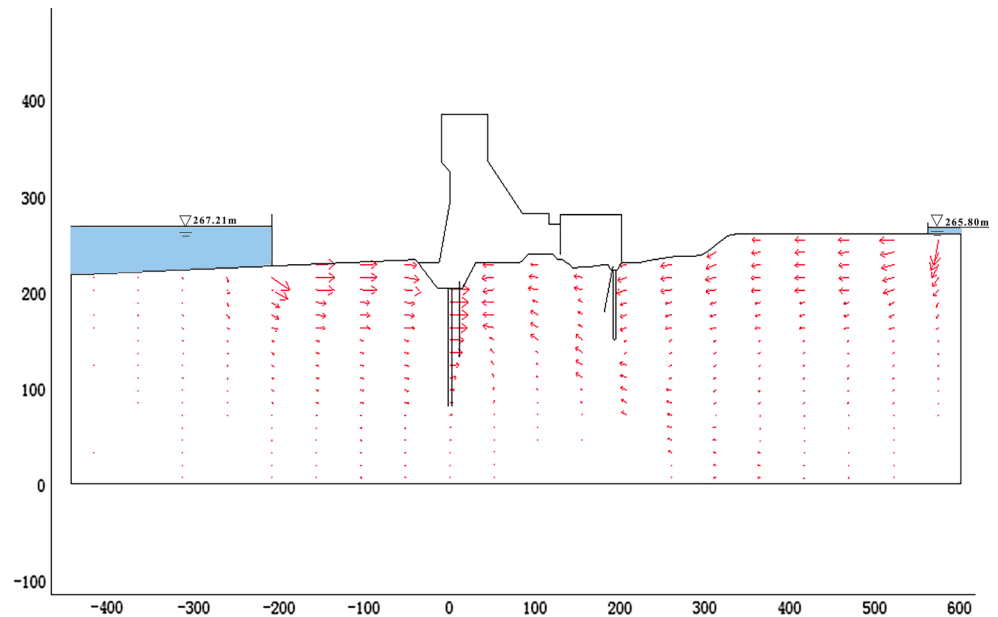
upstream corridor at a height of 210 m in the dam, especially from the channel section to the No. 11 flood discharge section. In addition, the corridor at 225 m near the left bank and that at 226 m height in the downstream portion of the dam plant and other areas also showed sporadic seepage/leakage. We collected water samples from each seepage/leakage point, the upstream side of the Jinsha River and from the groundwater on both sides for chemical analysis to investigate the water sources and possible effects on the dam foundation.

Water sampling and chemical characteristics of water

A total of 33 water samples were collected at three times from February 2008 to April 2008. All samples were collected into new polyethylene bottles after pumping for 10 min and then analysed within 2 weeks of sampling. Water samples were collected from the five following areas: (1) Jinsha River, at the upstream cofferdam (S1); (2) groundwater from the left and right bank, which was mixed and analysed as a composite to generate an average water quality index for groundwater on both sides of the bank (label S2); (3) seepage water from drilling areas in the corridors of the powerhouse sections (eight sections, No. 1–8) and the channel section (samples labelled as C1–C12); (4) seepage water from drilling areas in the corridors of the flood discharge section (thirteen sections, No. 1–13), from where 13 water samples were taken (X1–X13); (5) seepage water from the observation wells and drainage boreholes on the construction platform at both faces of the dam (an area known as the foundation pits; J1–J6). The sample locations are shown in Fig. 5 and the overall water quality characteristics are shown in Fig. 6.

As shown in Fig. 6, the water from Jinsha River was Ca–Na–Mg–HCO$_3$ type, while the groundwater on the side banks was Ca–Mg–Na–HCO$_3$–SO$_4$ type, indicating that it was similar to the river water, but contained SO$_4^{2-}$ in addition to HCO$_3^-$. Additionally, the overall seepage through different parts of the dam contained different levels of ionic components. Of the cations, Na$^+$ and K$^+$ dominated the water collected from seepage in the powerhouse and the flood discharge section, while in the pit the concentration of Ca^{2+} and Mg^{2+} increases. The main component of the seepage taken from the powerhouse and the flood discharge sections was HCO$_3^-$ + CO$_3^{2-}$, while the SO$_4^{2-}$ content was significantly higher in samples from the pit. The pH and TDS of the samples are shown in Fig. 7.

According to the pH, the water was neutral to weakly alkaline compared to the value of 7.14 of the sample from Jinsha River (S1), which is common among projects conducted in the region owing to the reaction with cement. The pH values of samples from the pit were lower. The minimum pH was 7.3, while that of water from the flood discharge section was 9.62 and that of samples from the powerhouse section was 8.26. The TDS of samples collected from the powerhouse section was between 220 and 430 mg/L, while in the flood discharge section it was between 330 and 1064 mg/L. The characteristics of the samples in the flood discharge section could be described as having both a high pH and a high TDS, while those from the powerhouse section and the pit were relatively low, which reflected the flow conditions to some extent. It should also be noted that the samples in nearby sections showed differences in range. For example, among samples collected from the pit, the maximum pH value was 8.82 while the minimum was 7.30. Similarly, the maximum

Fig. 5 Location of water samples
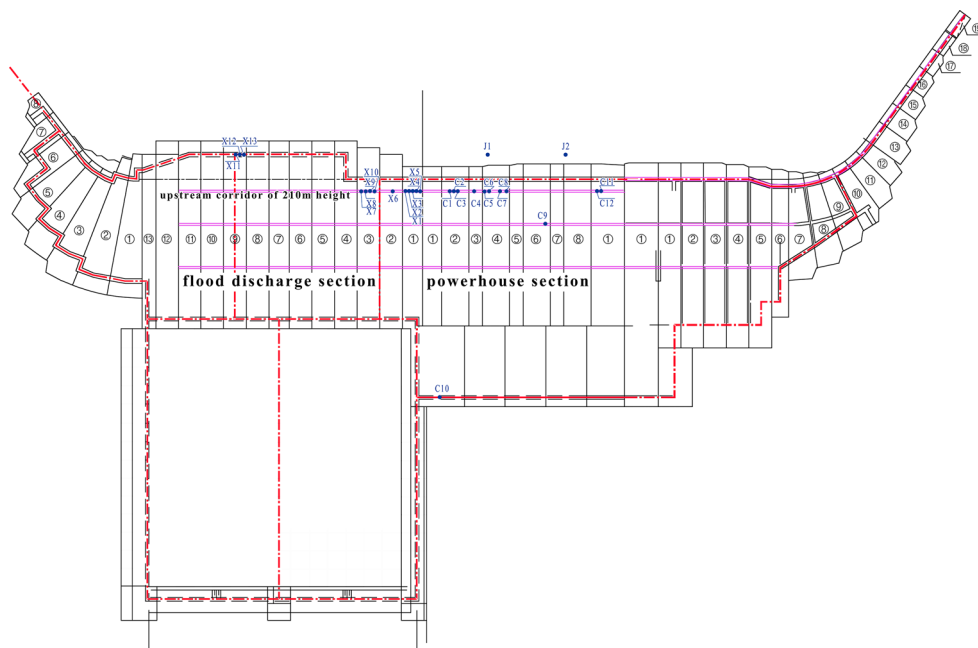
**Fig. 6** Piper plot of water samples from different dam sections
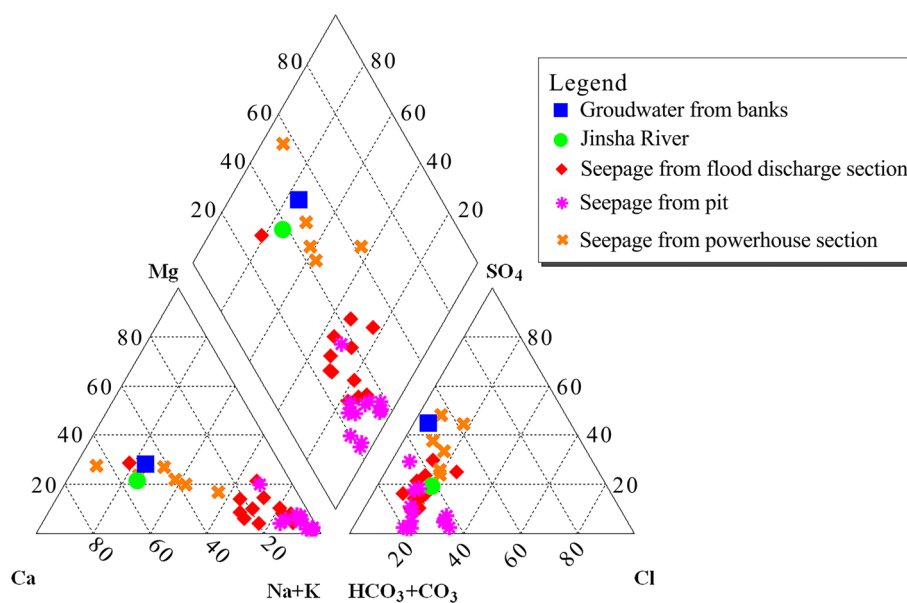
TDS of samples from flood discharge sections reached 1064 mg/L, while the minimum was only 330 mg/L. Therefore, these data cannot be divided simply according to their position in the dam when analysing the water quality and associated parameters such as flow conditions and supply sources.

Cluster analysis of water samples

Based on the aforementioned analyses, the chemical indices of samples from the same section showed little difference. Therefore, hierarchical cluster analysis (HCA) was used to classify the samples into several groups in each of which the samples have similar characteristics. HCA is a data classification technique commonly applied for classification of hydro-geochemical data. In HCA, sampling sites with the largest similarity are grouped, after which similar samples are joined with a linkage rule repeatedly until all observations have been classified. The samples in the same cluster have similar chemical characteristics that can reflect a certain type of flow, recharge and/or source condition. The results of HCA of the 33 groundwater samples are
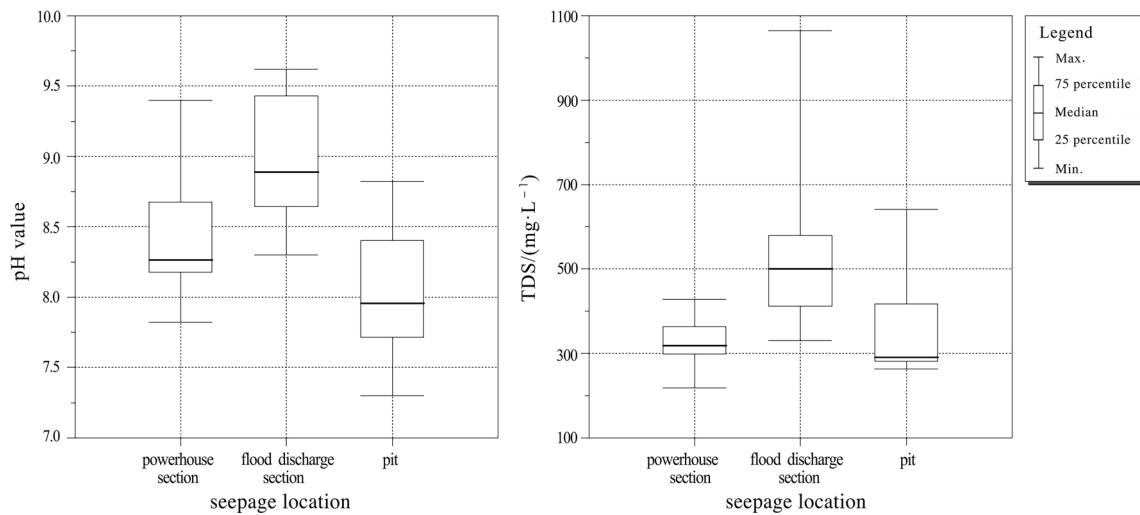
Fig. 7 *Box* plots of pH and TDS

Fig. 8 Dendrogram of the Q-mode hierarchical cluster analysis
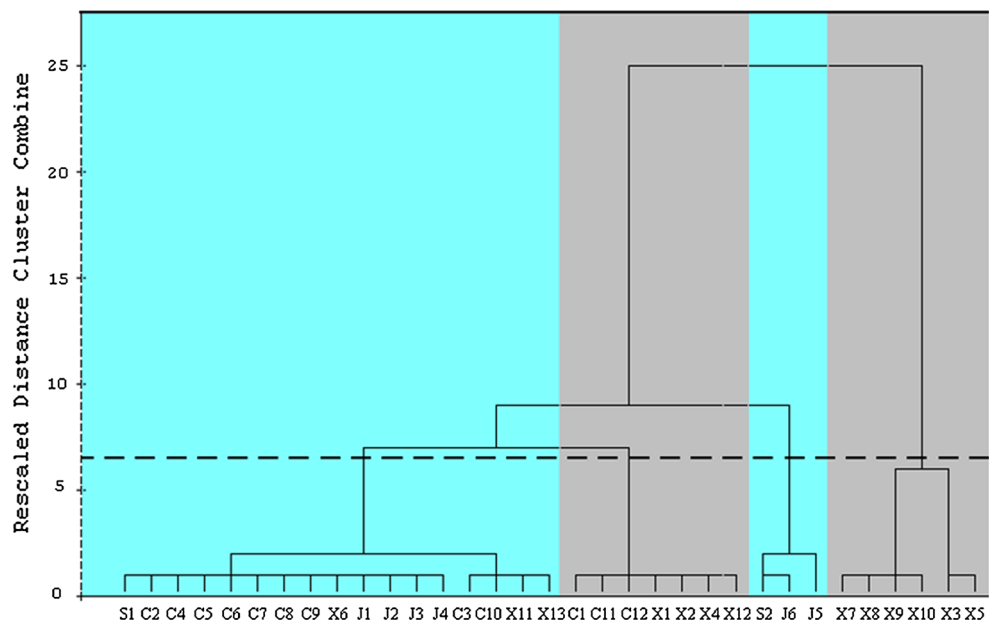
summarized in the dendrogram shown in Fig. 8, which uses Euclidean distance as a measure and Ward's method as a linkage rule to produce the most distinctive cluster groups as described by Belkhiri et al. (2012).

Based on the results shown in Fig. 8:

1. Four cluster groups were formed by drawing the phenon line at a standardized linkage distance of about seven across the dendrogram (L1–L4).
2. Cluster group L1 could be divided into two sub-groups, L1–1 and L1–2. The former contained the most samples of all groups (13), the majority of which were mainly from the powerhouse section and pit. It should be noted that the sample from the Jinsha River was

also found in this sub-group. Sub-group L1–2 consisted of four samples, mainly from the powerhouse section and flood discharge section.
3. There were seven samples in cluster group L2, three of which were from the powerhouse section and the remainder of which were from the flood discharge section.
4. Cluster group L3 contained only three samples, one from the riverbank groundwater and two from the pit leakage.
5. There were six samples in cluster group L4, which were all from the flood discharge section. This group was further divided into two sub-groups, L4–1 and L4–2.

Table 2 Mean values of chemical constituents of main cluster groups

	pH	Na$^+$	K$^+$	Ca^{2+}	Mg^{2+}	Cl$^-$	SO$_4^{2-}$	CO$_3^{2-}$	HCO$_3^-$	TDS
L1–1	8.182	63.804	8.713	28.637	10.458	31.433	60.081	0.512	192.804	300.041
L1–2	8.515	111.666	21.039	13.936	5.166	37.373	23.660	3.074	297.019	364.422
L2	9.146	128.371	24.186	9.843	5.669	38.681	53.020	50.947	199.427	410.429
L3	7.580	34.746	6.546	106.453	31.698	30.690	200.414	0.000	278.259	549.677
L4–1	9.480	207.150	39.028	7.161	1.761	117.068	22.732	106.067	195.407	598.671
L4–2	8.695	329.181	62.020	8.516	3.522	115.954	16.237	59.182	673.763	931.494

All indicators in mg/L (except pH values)

Table 2 presents the mean values of the geochemical data.

The results shown in Table 2 indicate the following:

1. The TDS increased from L1–1 to L4, with the mean value increasing from 300 to 931 mg/L.
2. The samples in group L1 had a low TDS and a slightly lower pH value. There were few differences between L1–1 and L1–2, although the former had a higher concentration of Ca^{2+}, Mg^{2+} and SO$_4^{2-}$ and a lower pH, Na$^+$, K$^+$, CO$_3^{2-}$ and HCO$_3^-$.
3. The samples in group L2 had a characteristically low TDS (410 mg/L) and a slightly higher pH (9.146).
4. There were only three samples in group L3, which was the fewest of all groups. Additionally, this group had the lowest pH, Na$^+$ and K$^+$ concentrations, while also having the highest Ca^{2+}, Mg^{2+} and SO$_4^{2-}$ concentrations among all groups.
5. The samples in group L4 had a high pH and TDS. All aqueous species in this group had higher concentrations of mineral elements than the other groups, except Ca^{2+}, Mg^{2+} and SO$_4^{2-}$.

Meanwhile the mineral saturation index of each group was also calculated, and the values of gypsum, anhydrite, dolomite and calcite were determined as indices of the extent of the reaction between groundwater and artificial building materials (Fig. 9).

As shown in Fig. 9, dolomite and calcite were supersaturated in all groups, while gypsum and anhydrite were not. Overall, the groups could be sorted by the sulphate saturation index as follows: L3 > L1 > L2 > L4. When sorted by carbonate, the groups were sorted as: L2 > L4 > L1 > L3.

Inverse modelling

There were interactions between the groundwater and solid phases such as aquifer minerals and the grout curtain in the dam foundation, which led to the observed changes in water quality. Inverse modelling was used to quantify the reactant amounts. Seepage water at the dam foundation originated from two sources, upstream of the Jinsha River
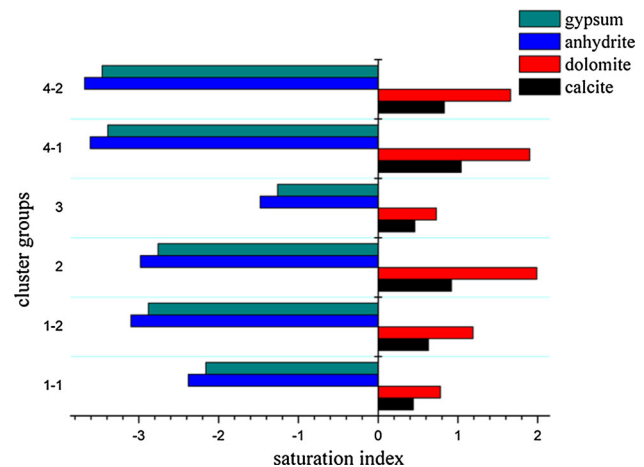
Fig. 9 Saturation indices for main groups

and groundwater from both banks. As shown in Table 1, the lithology of the dam foundation mainly included quartz, K-feldspar, plagioclase, clay minerals and a small amount of calcite and muscovite. Therefore, the main minerals modelled were K-feldspar, albite, anorthite, cement (Ca(OH)$_2$), CO$_2$(g), calcite, kaolinite, gypsum, illite and the cation exchange adsorption products of NaX and CaX$_2$ in the clays. The percentage of source water and reactants in each group were calculated by PHREEQC (Parkhurst and Appelo 1999), and the results are given in Table 3.

The results shown in Table 3 indicate:

1. Sub-groups L1–1 and L1–2 primarily originated from the upstream portion of the Jinsha River, with 86.01 and 69.77 %, respectively, originating from this source. The main dissolved minerals were anorthite and K-feldspar, which were accompanied by precipitation of illite and a small amount of ion exchange. Overall, dissolution was the main process in these two groups. No cement was involved in the reaction, indicating that the position from where these samples were collected was in good condition with respect to resistance to groundwater seepage.
2. Although there was a small amount of dissolution of feldspar minerals, precipitation was the main process

Table 3 Source ratio and quality of reactant minerals

	L1–1	L1–2	L2	L3	L4–1	L4–2
Percentage (%)						
S1	86.01	69.77	37.66	5.65	99.04	100
S2	13.99	30.23	62.34	94.35	0.96	0.00
Reactant (mol/L)						
Albite	0.000E+00	0.000E+00	0.000E+00	0.000E+00	0.000E+00	0.000E+00
Anorthite	2.140E−04	1.390E−03	1.730E−03	0.000E+00	1.400E−03	1.140E−03
K-feldspar	1.511E−04	9.814E−04	1.230E−03	0.000E+00	9.849E−04	8.027E−04
Calcite	–	–	−5.149E−04	–	–	–
Cement	0.000E+00	0.000E+00	0.000E+00	5.623E−04	5.461E−04	3.990E−03
CO_2 (g)	2.282E−04	1.810E−03	1.510E−03	1.340E−03	2.030E−03	9.040E−03
Kaolinite	0.000E+00	0.000E+00	0.000E+00	0.000E+00	0.000E+00	0.000E+00
Gypsum	0.000E+00	−4.968E−04	−5.147E−04	0.000E+00	−2.138E−04	−2.712E−04
Illite	−2.518E−04	−1.640E−03	−2.040E−03	0.000E+00	−1.640E−03	−1.340E−03
NaX	1.520E−03	3.710E−03	3.740E−03	0.000E+00	5.530E−03	1.170E−02
CaX_2	−7.598E−04	−1.850E−03	−1.870E−03	0.000E+00	−2.760E−03	−5.850E−03
Total (g/L)	1.954E−02	5.371E−02	−3.289E−03	1.006E−01	1.515E−01	7.174E−01

Positive numbers indicate dissolution, while negative numbers indicate precipitation

in group L2. The sources of feldspar were complex, with 37.66 % originating from the upstream portion of the river and 62.34 % from the groundwater, which may have caused precipitation.

3. Group L3 primarily originated from groundwater in the river bank, and the main reactant was cement. This was primarily because the two samples came from the shallow part of the pit and were thought to resemble the wastewater arising from construction.

4. Groups L4–1 and L4–2 contained all water samples from the flood discharge section, which were mainly from upstream of the Jinsha River. The reactants included the minerals and a larger dissolution amount of cement. This section contained a grout curtain wall to decrease the flow velocity, which permitted the full reaction between the water and artificial building materials.

Summary and conclusions

A variety of hydro-geochemical methods were used to reflect water–rock interactions during construction of Xiangjiaba Dam. Additionally, the sources of seepage water in drilling boreholes at the dam foundation were investigated by chemical analyses. Hydrochemistry diagrams were then drawn to evaluate the chemical characteristics of the water samples, after which a hierarchical clustering method was used to classify the samples according to their composition, and the average amount of

aqueous species was calculated. Finally, inverse modelling using PHREEQC was used to determine the amounts that each source contributed to each subdivision and the amount of each precipitation/dissolution mineral. These data were then used to determine if changes in the hydro-geological conditions occurred during construction. The results of the study can be summarized as follows:

1. Water samples from the same dam section may have shown differences in chemical characteristics in response to different seepage conditions.

2. Four main cluster groups (six sub-groups) were formed by the hierarchical clustering method.

3. The samples in group L1–1 and L3 had characteristically low TDS and pH values. In addition, the saturation indices of calcite and dolomite were lower than those of other groups. Based on inverse modelling, the amount of dissolution minerals in these two groups is small. Taken together, the results show that the seepage conditions of these two groups is relatively good and these places should be noticed during dam safety assessments.

Compared with operational hydropower stations, those under construction are complex with regards to their geotechnology. Additionally, monitoring data such as uplift and flow velocity are either absent or short-term during construction because monitoring equipment has not been installed or only run for a short period. Moreover, such data are easily affected by construction activities in this period. The results of this study showed that hydro-geochemical analysis of water samples from a typical dam

site was helpful in improving our understanding of the seepage conditions based on an understanding of the geological and hydro-geological conditions of the dam foundation.

References

Belkhiri L, Boudoukha A, Mouni L, Baouz T (2010) Application of multivariate statistical methods and inverse geochemical modeling for characterization of groundwater: a case study: Ain Azel plain (Algeria). Geoderma 159:390–398. doi:10.1016/j.geoderma.2010.08.016

Belkhiri L, Mouni L, Tiri A (2012) Water–rock interaction and geochemistry of groundwater from the Ain Azel aquifer. Algeria Environ Geochem Health 34:1–13. doi:10.1007/s10653-011-9376-4

Carucci V, Petitta M, Aravena R (2012) Interaction between shallow and deep aquifers in the Tivoli Plain (Central Italy) enhanced by groundwater extraction: a multi-isotope approach and geochemical modeling. Appl Geochem 27:266–280. doi:10.1016/j.apgeochem.2011.11.007

Chae G-T, Yun S-T, Kim K, Mayer B (2006) Hydrogeochemistry of sodium-bicarbonate type bedrock groundwater in the Pocheon spa area, South Korea: water–rock interaction and hydrologic mixing. J Hydrol 321:326–343. doi:10.1016/j.jhydrol.2005.08.006

Chae GT et al (2007) Fluorine geochemistry in bedrock groundwater of South Korea. Sci Total Environ 385:272–283. doi:10.1016/j.scitotenv.2007.06.038

Cloutier V, Lefebvre R, Therrien R, Savard MM (2008) Multivariate statistical analysis of geochemical data as indicative of the hydrogeochemical evolution of groundwater in a sedimentary rock aquifer system. J Hydrol 353:294–313. doi:10.1016/j.jhydrol.2008.02.015

Craft CD, Pearson RM, Hurcomb D (2007) Mineral dissolution and dam seepage chemistry–The Bureau of reclamation experience. In: Proceedings of the 2007 national meeting, Dam Safety

Craig I et al (2007) Evaporation, seepage and water quality management in storage dams: a review of research methods. Environ Health 7:84–97

Dassi L (2011) Investigation by multivariate analysis of groundwater composition in a multilayer aquifer system from North Africa: a multi-tracer approach. Appl Geochem 26:1386–1398. doi:10.1016/j.apgeochem.2011.05.012

El Naqa A, Al Kuisi M (2004) Hydrogeochemical modeling of the water seepages through Tannur Dam, southern Jordan. Environ Geol 45:1087–1100. doi:10.1007/s00254-004-0967-6

Gambillara R, Terrana S, Giussani B, Monticelli D, Roncoroni S, Martin S (2013) Investigation of tectonically affected groundwater systems through a multidisciplinary approach. Appl Geochem 33:13–24. doi:10.1016/j.apgeochem.2013.01.005

Ghobadi MH, Khanlari GR, Djalaly H (2005) Seepage problems in the right abutment of the Shahid Abbaspour dam, southern Iran. Eng Geol 82:119–126. doi:10.1016/j.enggeo.2005.09.002

Güler C, Thyne GD (2004) Hydrologic and geologic factors controlling surface and groundwater chemistry in Indian Wells-Owens Valley area, southeastern California, USA. J Hydrol 285:177–198. doi:10.1016/j.jhydrol.2003.08.019

Güler C, Thyne G, McCray J, Turner K (2002) Evaluation of graphical and multivariate statistical methods for classification of water chemistry data. Hydrogeol J 10:455–474. doi:10.1007/s10040-002-0196-6

Hussein M (2004) Hydrochemical evaluation of groundwater in the Blue Nile Basin, eastern Sudan, using conventional and multivariate techniques. Hydrogeol J 12:144–158. doi:10.1007/s10040-003-0265-5

Kim J-H, Kim R-H, Lee J, Cheong T-J, Yum B-W, Chang H-W (2005) Multivariate statistical analysis to identify the major factors governing groundwater quality in the coastal area of Kimje, South Korea. Hydrol Process 19:1261–1276. doi:10.1002/hyp.5565

Kumar M, Ramanathan AL, Rao MS, Kumar B (2006) Identification and evaluation of hydrogeochemical processes in the groundwater environment of Delhi, India. Environ Geol 50:1025–1039. doi:10.1007/s00254-006-0275-4

Kumar M, Kumari K, Singh U, Ramanathan AL (2009) Hydrogeochemical processes in the groundwater environment of Muktsar, Punjab: conventional graphical and multivariate statistical approach. Environ Geol 57:873–884. doi:10.1007/s00254-008-1367-0

Lee J-Y, Choi Y-K, Kim H-S, Yun S-T (2005) Hydrologic characteristics of a large rockfill dam: Implications for water leakage. Eng Geol 80:43–59. doi:10.1016/j.enggeo.2005.03.002

Lee J, Kim H, Yun S, Kwon J (2009) Factor and cluster analyses of water Chemistry in and around a large Rockfill Dam: implications for water leakage. J Geotech Geoenviron Eng 135:1254–1263. doi:10.1061/(ASCE)GT.1943-5606.0000039

Lin CY, Musta B, Abdullah MH (2013) Geochemical processes, evidence and thermodynamic behavior of dissolved and precipitated carbonate minerals in a modern seawater/freshwater mixing zone of a small tropical island. Appl Geochem 29:13–31. doi:10.1016/j.apgeochem.2012.10.029

Ma R, Wang Y, Sun Z, Zheng C, Ma T, Prommer H (2011) Geochemical evolution of groundwater in carbonate aquifers in Taiyuan, northern China. Appl Geochem 26:884–897. doi:10.1016/j.apgeochem.2011.02.008

Mahlknecht J, Steinich B, de León IN (2004) Groundwater chemistry and mass transfers in the Independence aquifer, central Mexico, by using multivariate statistics and mass-balance models. Environ Geol 45:781–795. doi:10.1007/s00254-003-0938-3

Monjerezi M, Vogt RD, Aagaard P, Saka JDK (2011) Hydrogeochemical processes in an area with saline groundwater in lower Shire River valley, Malawi: an integrated application of hierarchical cluster and principal component analyses. Appl Geochem 26:1399–1413. doi:10.1016/j.apgeochem.2011.05.013

Nusier O, Alawneh A, Malkawi A (2002) Remedial measures to control seepage problems in the Kafrein dam, Jordan. Bull Eng Geol Environ 61:145–152. doi:10.1007/s100640100131

Parkhurst DL, Appelo CAJ (1999) User's guide to PHREEQC (Version 2)-A computer program for speciation, batch-reaction, one-dimensional transport, and inverse geochemical calculations

Peng T-R, Wang C-H (2008) Identification of sources and causes of leakage on a zoned earth dam in northern Taiwan: hydrological and isotopic evidence. Appl Geochem 23:2438–2451. doi:10.1016/j.apgeochem.2008.05.015

Rosenthal E, Zilberbrand M, Livshitz Y (2007) The hydrochemical evolution of brackish groundwater in central and northern Sinai (Egypt) and in the western Negev (Israel). J Hydrol 337:294–314. doi:10.1016/j.jhydrol.2007.01.042

Salifu A, Petrusevski B, Ghebremichael K, Buamah R, Amy G (2012) Multivariate statistical analysis for fluoride occurrence in groundwater in the Northern region of Ghana. J Contam Hydrol 140–141:34–44. doi:10.1016/j.jconhyd.2012.08.002

Sharif MU, Davis RK, Steele KF, Kim B, Kresse TM, Fazio JA (2008) Inverse geochemical modeling of groundwater evolution

with emphasis on arsenic in the Mississippi River Valley alluvial aquifer, Arkansas (USA). J Hydrol 350:41–55. doi:10.1016/j.jhydrol.2007.11.027

Srivastava S, Ramanathan AL (2008) Geochemical assessment of groundwater quality in vicinity of Bhalswa landfill, Delhi, India, using graphical and multivariate statistical methods. Environ Geol 53:1509–1528. doi:10.1007/s00254-007-0762-2

Stüben D, Berner Z, Chandrasekharam D, Karmakar J (2003) Arsenic enrichment in groundwater of West Bengal, India: geochemical evidence for mobilization of As under reducing conditions. Appl Geochem 18:1417–1434. doi:10.1016/S0883-2927(03)00060-X

Sung K-Y, Yun S-T, Park M-E, Koh Y-K, Choi B-Y, Hutcheon I, Kim K-H (2012) Reaction path modeling of hydrogeochemical evolution of groundwater in granitic bedrocks, South Korea. J Geochem Explor 118:90–97. doi:10.1016/j.gexplo.2012.05.004

Unal B, Eren M, Yalcin MG (2007) Investigation of leakage at Ataturk dam and hydroelectric power plant by means of hydrometric measurements. Eng Geol 93:45–63. doi:10.1016/j.enggeo.2007.02.006

Uromeihy A, Farrokhi R (2012) Evaluating groutability at the Kamal-Saleh Dam based on Lugeon tests. Bull Eng Geol Environ 71:215–219. doi:10.1007/s10064-011-0382-7